R. & M. No. 3137
(20,238)
A.R.C. Technical Report

R. & M. No. 3137

MINISTRY OF AVIATION

AERONAUTICAL RESEARCH COUNCIL
REPORTS AND MEMORANDA

The Calculation of Lift Slopes, Allowing for Boundary Layer, with Applications to the RAE 101 and 104 Aerofoils

By D. A. Spence and J. A. Beasley

LONDON: HER MAJESTY'S STATIONERY OFFICE
1960
SEVEN SHILLINGS NET

The Calculation of Lift Slopes, Allowing for Boundary Layer, with Applications to the RAE 101 and 104 Aerofoils

By D. A. Spence and J. A. Beasley

Communicated by the Director-General of Scientific Research (Air)
Ministry of Supply

*Reports and Memoranda No. 3137**
February, 1958

Summary. The need to know two-dimensional low-speed characteristics accurately in designing swept-back wings for transonic aircraft has led to a revival of interest in calculations of the loss of lift below the ideal-flow value caused by the boundary layer.

The existing methods[1,2] for performing this calculation have now been reduced to a straightforward routine. This is sufficiently sensitive for coefficients to be evaluated at rather small incidences, *e.g.*, $\alpha = 2$ deg, for which the boundary-layer part of the calculation is tractable; from these results the lift at higher incidences may be estimated.

The method has been applied to RAE 101 and 104 sections of 6, 10 and 15 per cent thickness at $R = 10^6$, 10^7 and 10^8 with a wide range of transition positions. Good agreement exists between prediction and measurement for the 10 per cent thick 101 section tested by Brebner and Bagley[13]. The predictions have also been compared with those of the Royal Aeronautical Society data sheet Wings 01.01.05[14], but the measure of agreement in this case lies just outside the assessed accuracy of the data sheet. Although the discrepancies are not fully accounted for, they may be due in part to over-simplification of the effects of transition and incidence on the data sheet, and the present method should, it is thought, yield accurate results when the correct transition positions are used.

An Appendix shows that circulation in the wake, which is treated as zero in Refs. 1 and 2, leads to reduction of lift by a factor estimated as $1 - 0{\cdot}214\sqrt{C_D}$ (C_D = drag coefficient); this has not been taken into account in these calculations, since C_D is of the order of $0{\cdot}005$.

1. *Introduction.* 1.1. *Outline of Method.* In Ref. 1, which followed the work of Preston[2], the theory was given of a method for calculating the amount by which the boundary layer and wake reduce the lift of a two-dimensional aerofoil below that given by ideal-flow theory. The ultimate object of such calculations is to produce generalised curves predicting the influence of Reynolds number on lift for given transition positions, thickness/chord ratios and trailing-edge angles†, comparable to those for drag given by Squire and Young[3] in 1938. Mention should be made of a paper in which Sears[4] in 1956 has reviewed developments in this field. At the Royal Aircraft Establishment the work has recently received stimulus from the need to know two-dimensional lift slopes accurately in designing swept-back wings for transonic aircraft.

* R.A.E. Report Aero. 2598, received 13th June, 1958.

† In fact it was found that the lift reduction factors for different shapes could be collapsed on the basis of trailing-edge angle alone, although the inviscid lift coefficient depends mainly on the thickness/chord ratio.

The calculation of lift is more complicated than that of drag, since it requires iteration between (i) the calculation of the boundary-layer thickness for a given pressure distribution, and (ii) the calculation of circulation and hence pressure distribution when the boundary-layer thickness is known. Early attempts to apply the method of Ref. 1 at incidences α of 6 and 10 deg brought to light a considerable difficulty in the boundary-layer part of the calculation. It was found that the existing methods for calculating the growth of turbulent boundary layers broke down in the severe adverse pressure gradients, sometimes associated with laminar separation bubbles, which develop behind the suction peak of a thin aerofoil at these incidences. It then appeared that it would not be possible to calculate boundary-layer effects on lift with any confidence until a more satisfactory theory was available for boundary-layer growth in such conditions, and no such theory is yet in sight.

However, the lift is proportionately reduced below its ideal value even at the smallest incidences. Attempts were therefore made to estimate the lift slope at zero incidence, namely, $a_1 = (\partial C_L/\partial\alpha)_{\alpha=0}$, by calculating lift reduction factors at $\alpha = 2$ deg. It was found that for the less severe adverse gradients which then occur the boundary-layer calculations are quite practicable, and sufficiently sensitive to enable the circulation to be calculated accurately. Moreover, the steps in the calculation are much simplified, and the method can be reduced to a straightforward routine.

The percentage of the ideal lift developed, namely, a_1/a_0, has been calculated for the RAE 101 and 104 aerofoils tabulated by Pankhurst and Squire[5], with thickness/chord ratios of 6, 10 and 15 per cent in each case, at Reynolds numbers 10^6, 10^7 and 10^8. A range of transition positions x_{Tu}, X_{Tl} between 0 and 80 per cent chord on upper and lower surfaces was used. The majority of the calculations were made with $\alpha = 2$ deg, but a few cases with $\alpha = 4$ deg and 6 deg are included for comparison.

1.2. *Transition Positions.* The location of transition was treated as an external parameter since in practice it may be governed by factors which do not enter the calculation directly, such as surface finish, sweepback and turbulence level.

These extraneous factors being fixed, however, the free transition point is likely to depend on both Reynolds number and pressure distribution; the latter depends on incidence, so we may expect both x_{Tu} and x_{Tl} to be functions of both α and R. By symmetry $x_{Tu} = x_{Tl}$ when $\alpha = 0$ (or if not, the asymmetry in transition creates a lift even at zero incidence, as on a swinging cricket ball), but in general the transition points are different.

As incidence is increased the transition position on the upper surface moves forward, and that on the lower surface moves aft. It will be shown that if $x_{Tl} - x_{Tu}$ is increased the loss of lift factor increases too, and this effect is demonstrated in the experimental results of Ref. 13 (For example, in Fig. 10 of that report, C_L/C_{L0} decreases by 8 per cent, from 0·9 to 0·8, as C_L increases from 0 to 1).

On the other hand, if transition is fixed over a range of incidence the evidence of Ref. 13 is that the lift curve slope tends to remain constant. In this case it should be possible to estimate the lift at an incidence α other than 2 deg from the value of a_1/a_0 obtained by the 2 deg calculation simply as a_1/a_0 multiplied by αa_0.

1.3. *Effect of Wake Circulation.* The theory of Refs. 1 and 2 rested on the assumption, originating in a conjecture of G. I. Taylor[6], that the circulation round any circuit enclosing the aerofoil and cutting the streamlines in the wake at right angles was constant, and hence that the circulation round a circuit crossing the wake in this manner at the trailing edge and at infinity downstream was

zero. When the theory of the jet-flap system was studied, it became clear (Preston[7]) that this assumption was not in general correct, since the wake represents a stream of air with reduced momentum turning through a finite angle α between the trailing edge and infinity. In the appendix it is shown that the resulting circulation in the wake, of amount $\alpha c U_\infty C_D$, reduces the lift by a factor estimated as $1 - 0{\cdot}214\sqrt{C_D}$, where C_D is the drag coefficient. For the 10 per cent thick RAE 101 section, C_D is less than $0{\cdot}008$ up to 4 deg incidences, and this factor has not been applied in the present calculations.

It should also be remarked that in Refs. 1 and 2 the boundary condition which fixes the circulation is applied at the edge of the boundary layers just above and just below the trailing edge, whereas in fact it should be applied along the whole of the wake, as was done in the inviscid linearised treatment of the jet flap by Spence[15]. A full discussion of the nature of the simplifications used is to be given by Maskell in an R.A.E. report to be issued.

2. *Theory of Potential-Flow Calculations.* For convenience an outline is given in this Section of the theory described more fully in Ref. 1.

2.1. *Conformal Transformations.* The flow outside the boundary layer and wake is effectively inviscid, and may be obtained from a potential-flow calculation in which these regions are represented by source distributions equal in magnitude to the streamwise rate of change of their displacement fluxes* and located on the surface and on the wake centre-line. The circulation is then found from the consideration that the velocity in the main streams should be the same at the outer edges of both upper and lower boundary layers at the trailing edge (and all along the wake). This follows from the approximate constancy of static pressure across the wake. The stages in the calculation are indicated in Fig. 1, which shows the physical (z) plane, the ζ plane in which the aerofoil is transformed into a slit from 0 to a on the real axis, and the Z plane in which the aerofoil and slit correspond to a circle of radius $a/4$.

The points P_1, P_2 at the edges of the boundary layers are given by†

$$\left.\begin{aligned} z &= 1 + \delta^{(1)}\, e^{i(\pi/2-\tau/4)} &&= 1 + \delta^{(1)}\, e^{i\pi(\omega/4)} \\ z &= 1 + \delta^{(2)}\, e^{-i(\pi/2-\tau/4)} &&= 1 + \delta^{(2)}\, e^{-i\pi(\omega/4)} \end{aligned}\right\}. \tag{1}$$

respectively, where $\delta^{(1)}$, $\delta^{(2)}$ are the thicknesses of upper and lower boundary layers, τ is the trailing-edge angle, and

$$\omega = 2 - \frac{\tau}{\pi}. \tag{2}$$

In the circle plane, these points may be written

$$Z = \frac{a}{4}\, e^{(1+i)\lambda_1}, \qquad Z = \frac{a}{4}\, e^{(1-i)\lambda_2} \tag{3}$$

---

* Displacement flux $= \int_0^\delta (U_1 - U)\, dy = U_1\delta_1$.

† Raised suffixes are used to avoid confusion with the notation δ_1, δ_2 for displacement and momentum thicknesses. Except with symbol δ, lower suffixes $_{1,2}$ refer to the upper and lower points P_1, P_2.

respectively, correct to $0(\lambda^2)$, and in the slit plane, which is connected to the circle by

$$\zeta = Z + \frac{a^2}{16Z} + \frac{a}{2} \tag{4}$$

they are

$$\zeta = a\left(1 + \frac{i\lambda_1^2}{2}\right), \qquad \zeta = a\left(1 - \frac{i\lambda_2^2}{2}\right), \tag{5}$$

ignoring terms of order λ^4.

The transformation between the ζ and z planes may be written, in the trailing edge neighbourhood, in the Schwarz-Christoffel form

$$\frac{\zeta}{a} - 1 = A\,(z - 1)^{2/\omega}. \tag{6}$$

A convenient method for evaluating the constant A (and at the same time calculating the velocity on the aerofoil surface, which is required in the boundary-layer part of the calculation) has been given by Spence and Routledge[8], λ_1 and λ_2 may then be obtained from known values of $\delta^{(1)}$, $\delta^{(2)}$ by the relation

$$\lambda^2 = 2A\,\delta^{2/\omega}. \tag{7}$$

Values of A are found to be between 0·9 and 1, and a good approximation is given by

$$A = 1 - 0{\cdot}65\frac{t}{c} \tag{8}$$

(t/c being the thickness/chord ratio).

2.2. *Calculation of Circulation.* We write the circulation as $(1 - \gamma)$ times the Kutta-Joukowski value $4\pi \sin\alpha$ (α = incidence) and our aim is to obtain an equation for γ. For the low incidences, and hence relatively thin boundary layers, of the present investigation squares of λ will be omitted.

The complex velocity potential of flow with incidence α, unit velocity at infinity, and $(1 - \gamma)$ times the Joukowski circulation, past a circle of radius $a/4$ in the Z plane, is

$$\omega = \phi + i\psi = Z\,e^{-i\alpha} + \left(\frac{a}{4}\right)^2 \frac{1}{Z} e^{i\alpha} + 2i \sin\alpha(1 - \gamma)\frac{a}{4}\log Z. \tag{9}$$

Differentiating this expression and equation (4), it follows that the complex velocity in the slit plane is then, to the same order of accuracy as equation (5)

$$\frac{d\omega}{d\zeta} = \left\{\frac{4Z}{a} e^{-i\alpha} - \frac{a}{4Z} e^{i\alpha} + (1 - \gamma)2i \sin\alpha\right\} \Big/ \left(\frac{4Z}{a} - \frac{a}{4Z}\right). \tag{10}$$

For a point P_1 for which $Z = \frac{a}{4} e^{(1+i)\lambda}$ this reduces to

$$\frac{d\omega}{d\zeta} = \cos\alpha - i \sin\alpha\,\{\cosh(1 + i)\lambda - (1 - \gamma)\}/\sinh(1 + i)\lambda. \tag{11}$$

Expanding in powers of λ up to λ^4 (11) becomes

$$\frac{d\omega}{d\zeta} = \cos\alpha - \frac{\sin\alpha}{2\lambda}\left[\left\{\gamma + \frac{\lambda^4}{6} - \lambda^2\left(1 - \frac{\gamma}{3}\right)\right\} + i\left\{\gamma + \frac{\lambda^4}{6} + \lambda^2\left(1 - \frac{\gamma}{3}\right)\right\}\right]. \tag{12}$$

Now, in calculations it is invariably found that γ/λ is of order unity, and that λ is of order $0{\cdot}1$, so that, excluding as before terms of order λ^2, the tangential velocity component in the ζ plane due to circulatory flow is

$$\mathscr{R}\frac{d\omega}{d\zeta} = \cos\alpha - \tfrac{1}{2}\sin\alpha\left(\frac{\gamma}{\lambda} - \lambda\right). \tag{13}$$

The corresponding expression for the lower-surface point $Z = (a/4)\,e^{(1-i)\lambda}$ is obtained by changing the sign of α, *i.e.*, to

$$\mathscr{R}\frac{d\omega}{d\zeta} = \cos\alpha + \frac{1}{2}\sin\alpha\left(\frac{\gamma}{\lambda} - \lambda\right). \tag{14}$$

We may now suppose that the effect of the source distribution which represents the boundary layer and wake is to produce, in the ζ plane, an additional velocity component Δu at the point in question. The procedure for calculating Δu from the distribution of displacement thickness is given in Section 3.5 below. The total tangential velocity components in the ζ plane at the points corresponding to P_1 and P_2 may then be written

$$\left.\begin{aligned}\cos\alpha - \frac{1}{2}\sin\alpha\left(\frac{\gamma}{\lambda_1} - \lambda_1\right) + \Delta u_1\\ \cos\alpha + \frac{1}{2}\sin\alpha\left(\frac{\gamma}{\lambda_2} - \lambda_2\right) + \Delta u_2\end{aligned}\right\} \tag{15}$$

respectively. To convert these to the corresponding velocity components in the z plane, one must multiply them by the modulus of transformation, which is given by

$$\left|\frac{d\zeta}{dz}\right| = \text{const} \times |\zeta - a|^{\tau/2\pi} \qquad \text{(from (6), (2))} \tag{16}$$

$$= \text{const} \times \lambda^{\tau/\pi} \qquad \text{(from (5))}. \tag{17}$$

Thus the tangential velocity at P_1 in the aerofoil plane is

$$q_1 = \text{const} \times \lambda_1^{\tau/\pi}\left\{\cos\alpha - \frac{1}{2}\sin\alpha\left(\frac{\gamma}{\lambda_1} - \lambda_1\right) + \Delta u_1\right\} \tag{18}$$

and that at P_2 is

$$q_2 = \text{const} \times \lambda_2^{\tau/\pi}\left\{\cos\alpha + \frac{1}{2}\sin\alpha\left(\frac{\gamma}{\lambda_2} - \lambda_2\right) + \Delta u_2\right\} \tag{19}$$

(The constants in (18) and (19) are the same).

Since the static pressures and total heads at P_1 and P_2 are the same, these two velocities may be equated and, for small α, we obtain the following equation for γ:

$$\frac{\alpha}{2}\left(\frac{1}{\lambda_1} + \frac{1}{\lambda_2}\right)\gamma = \left(\frac{\lambda_1}{\lambda_2}\right)^{\tau/\pi} - 1 + \frac{\alpha}{2}(\lambda_1 + \lambda_2) + (\Delta u_1 - \Delta u_2). \tag{20}$$

This is the basic equation for calculating the defect in lift, since

$$\frac{C_L}{C_{L0}} = 1 - \gamma. \tag{21}$$

If the lift vanishes at zero incidence (*i.e.*, if the transition points are then the same on both surfaces, and the aerofoil is symmetrical), equation (21) is the ratio of the real and ideal lift slopes, namely, a_1/a_0.

3. *Calculation of Boundary-Layer Thickness.* 3.1. *External Velocity Distribution.* The velocity distribution used in calculating the boundary-layer growth was that given by inviscid-flow theory over the greater part of the aerofoil surface (strictly, the velocity distribution should be modified for boundary-layer effects but this was found not to produce a significant change in a_1/a_0). Near the trailing edge the theoretical surface velocity vanishes and the relevant velocity in this region is that at the edge of the boundary layer, *i.e.*, q_1 or q_2 in the notation of the previous Section. This velocity could be found by iteration and the following geometrical method was used to obtain a first approximation. Straight lines were constructed tangential to the upper and lower-surface velocity distributions at 85 per cent chord. The velocity at the trailing edge was then assumed to be given by the point midway between these two lines at the trailing edge, and the velocity distribution between 85 per cent chord and the trailing edge was assumed to be linear. This procedure is illustrated in Fig. 2. The velocity distribution thus obtained could then be used to calculate the boundary-layer thickness and hence the reduction of lift factor a_1/a_0. A new trailing-edge velocity was then calculated from equation (18) using this value of a_1/a_0 and one such iteration was usually found to be sufficient. For the RAE 101 and 104 aerofoils it was found that the values of a_1/a_0 calculated from the first rough approximations of trailing-edge velocity differed very little from those calculated from the more accurate approximations. The calculation of the boundary layer was thus greatly simplified.

3.2. *Momentum Thickness.* The momentum thickness was calculated using the integrals obtained by Thwaites[9] for laminar layers and by Spence[10] for turbulent layers. These are respectively

$$\text{(laminar flow)} \qquad \left(\frac{U}{U_\infty}\right)^6 \left(\frac{\delta_2}{c}\right)^2 = \frac{0{\cdot}45}{R} \int_{x_s/c} \left(\frac{U}{U_\infty}\right)^5 d\left(\frac{x}{c}\right), \tag{22}$$

where $R = U_0 c/\nu$ and x_s denotes the forward stagnation point (x being measured along the surface), and

$$\text{(turbulent flow)} \qquad \left(\frac{U}{U_\infty}\right)^{4{\cdot}2} \left(\frac{\delta_2}{c}\right)^{1{\cdot}2} = \frac{0{\cdot}0106}{R^{0{\cdot}2}} \int_{x_T/c} \left(\frac{U}{U_\infty}\right)^4 d\left(\frac{x}{c}\right) + \text{const}, \tag{23}$$

where x_T denotes the assumed transition point. The constant is then the value of the left-hand side at this point, where it is assumed that δ_2 is continuous, its value being obtained from the laminar boundary-layer calculations.

3.3. *Displacement Thickness.* The displacement thickness was obtained from the momentum thickness by assuming the shape parameter, H, to have the constant value $1{\cdot}4$. This should be fully justifiable for the adverse pressure gradients occurring at the small incidences (2 deg and 4 deg) for which the calculations were made. Thus, with δ_2 calculated as above,

$$\delta_1 = 1{\cdot}4\delta_2 . \tag{24}$$

3.4. *Boundary-Layer Thickness at Trailing Edge.* The total thickness of the boundary layer at the trailing edge, which is required in order to locate the points P_1 and P_2, is obtained from the relation

$$\frac{\delta}{\delta_2} = \frac{H(H+1)}{(H-1)}, \tag{25}$$

which holds for power-law velocity profiles. With $H = 1{\cdot}4$ this gives

$$\delta = 8{\cdot}4\delta_2 . \tag{26}$$

3.5. *Wake Thickness.* To calculate the velocity aft of the trailing edge would be very complicated, and in any case uncertain because the circulation is not known at this stage. We have therefore used instead an arbitrary approximation, by assuming that the upper-surface velocity distribution is symmetrical ahead of and behind the trailing edge up to the point where the free-stream velocity is reached, *i.e.*,

$$U_{(c-x)} = U_{(c+x)} , \tag{27}$$

where $U \leqslant U_\infty$. The velocities above and below the wake are assumed equal. In practice $U_{\text{T.E.}}/U_\infty$ is between $0{\cdot}9$ and $1{\cdot}0$ so that at worst the error involved is small.

The momentum thickness of the wake was obtained from the thickness at the trailing edge and the assumed velocity distribution by means of the relation

$$\frac{\delta_2}{c}\left(\frac{U}{U_\infty}\right)^{3{\cdot}4} = \text{const} , \tag{28}$$

which is an approximate integral of the momentum equation.

The decay of H was calculated from the equation given in Ref. 11, namely,

$$1 - \frac{1}{H} = \left(1 - \frac{1}{H_1}\right)\left(1 + 40\,\frac{x}{c}\right)^{-1/2} , \tag{29}$$

where H_1 is the value of H at the trailing edge, from which x is measured. In the present case, $H_1 = 1{\cdot}4$ and

$$\frac{1}{H} = 1 - \frac{2}{7}\left(1 + 40\,\frac{x}{c}\right)^{-1/2} \tag{30}$$

(an alternative would have been to use the empirical formula

$$H - 1 = (H_1 - 1)\, ln\,(U/U_\infty)/\, ln\,(U_1/U_\infty)$$ of Squire and Young[3]).

Δu_1 and Δu_2 were then calculated from the equation given in Ref. 1, *i.e.*,

$$\Delta u = \frac{1}{\pi}\int_{-\pi/2}^{\pi/2}\left(\frac{\psi^*}{\psi_{\text{T.E.}}}\right)\cos 2\chi\, d\chi , \tag{31}$$

where $\psi^* = H\delta_2 U$, $\psi_{\text{T.E.}} = 8{\cdot}4(\delta_2 U)_{\text{T.E.}}$ and χ is a parameter, introduced to simplify the computation, defined by $\phi = \phi_T + \psi_1 \tan\chi$. The values of ϕ and ψ at the point P_1 are ϕ_T and ψ_1.

4. *Calculations Performed.* The method has been used to compute $\gamma = 1 - (a_1/a_0)$ for RAE 101 and 104 aerofoils of thickness/chord ratios 6, 10 and 15 per cent at Reynolds numbers, based on chord length, of 10^6, 10^7 and 10^8. For RAE 101 calculations were made with transition points at 0, 10, 50, 65 and 80 per cent chord (with $x_{Tu} \leqslant x_{Tl}$ in each case), and for RAE 104 with transition at 10 per cent chord. A number of values of γ so obtained are given in Table 1.

The method was also used to compute γ for the 10 per cent thick RAE 101 aerofoil at incidences of 4 deg and 6 deg, at a Reynolds number of 10^6 and transition points at 0 and 50 per cent chord. Because of the severe adverse pressure gradient behind the forward peak the method could not be

used for the 6 deg case with any confidence, but the resulting values of γ, tabulated in Table 1, suggest that in this particular case 6 deg is not outside the scope of the method.

The effects of Reynolds number, trailing-edge angle, transition position and incidence may be summarized as follows:

4.1. *Reynolds Number.* In every case (Figs. 3 to 7) the loss of lift decreases with increase of R, the asymptotic value for $R \to \infty$ being of course $\gamma = 0$.

4.2. *Trailing-Edge Angle.* Values of $\{1 - (a_1/a_0)\}$ for both section shapes are compared in Fig. 3. They are plotted against thickness/chord ratio and against tan $\frac{1}{2}\tau$; in the latter case it is seen that for a given Reynolds number the calculated points for both aerofoils tend to lie on one smooth curve. This suggests that the aerofoil shapes could be fairly well correlated in terms of trailing-edge angle alone, as was expected from the analysis of Ref. 1. The loss in lift increases with τ.

4.3. *Transition Positions.* The effect of changes in transition position is illustrated in Figs. 4, 5 and 7, the data being calculated for the 101 section only. For plotting Figs. 6 to 9 the ratio C_L/C_{L0} of the calculated and ideal lift coefficients at $\alpha = 2$ deg has been used in the ordinate, in preference to a_1/a_0. This is because, with fixed unsymmetrical transition positions, the no-lift angle would differ from zero, and we could not estimate a_1 by C_L/α.

(*a*) *Symmetrical positions.* Figs. 4 and 5 refer to cases in which transition occurs at the same point on both surfaces: in Fig. 4, a_1/a_0 is plotted against tan $\frac{1}{2}\tau$ (hence permitting the data to be used for other aerofoil shapes), for $x_T/c = 0$, $0{\cdot}1$ and $0{\cdot}5$ at the three Reynolds numbers, while in Fig. 5, a_1/a_0 for the 10 per cent thick section only is plotted against x_T/c for the range $0 \leqslant x_T/c \leqslant 0{\cdot}8$. From both Figures it is seen that a rearward movement of the (symmetrical) transition point reduces the loss in lift.

(*b*) *Unsymmetrical positions.* Figs. 7a, 7b and 7c show the effect of variations of upper transition point, when the lower point is fixed, at $(x_T/c)_l = 0{\cdot}50$, $0{\cdot}65$, $0{\cdot}80$ respectively. It is seen that the further the upper transition point is ahead of the lower, the greater is the loss of lift $1 - C_L/C_{L0}$. It was found that for all three sets of curves and for both Reynolds numbers shown, the effect of the asymmetry could be approximated by the linear relation

$$C_L = (C_L)\text{symmetrical transition} - m\left(\frac{x_{Tl} - x_{Tu}}{c}\right). \tag{32}$$

In our case of tan $\frac{1}{2}\tau = 0{\cdot}0895$ and $\alpha = 2$ deg, $m = 0{\cdot}13620$. This relation is of the same form as one found from experimental data at zero incidence by Bryant and Garner[12].

4.4. *Incidence.* Fig. 6a shows that with symmetrical fixed transition positions a_1/a_0 is nearly constant over the range 2 to 6 deg. This is consistent with the observations of Brebner and Bagley in Ref. 13. For the case $x_{Tu}/c = 0$, $x_{Tl}/c = 0{\cdot}5$, a_1/a_0 is seen to increase with incidence so that the value of a_1/a_0 for a given pair of transition positions at 2 deg may be the same as that for a different pair of transition positions at 6 deg. This illustrates the mechanism by which a_1/a_0 remains nearly constant with incidence even though the transition positions change considerably.

5. *Comparison with Experimental Results of Ref.* 13. The tests by Brebner and Bagley on a 10 per cent thick RAE 101 section at $R = 1{\cdot}7 \times 10^6$ and $R = 3{\cdot}4 \times 10^6$ allow a direct comparison with the present results. This has been carried out for $\alpha = 2$ deg, using the observed points for both free and fixed transition and the agreement, shown in Fig. 8, is good in both cases.

In Fig. 8a the results in the transition-fixed case, for which $x_T/c = 0{\cdot}15$ on both surfaces, are compared with a curve of a_1/a_0 against $\log_{10} R$ obtained by cross-plotting Fig. 5 at this value of x_T/c.

In Fig. 8b the free transition case is shown. The observed transition points were: at $R = 1{\cdot}7 \times 10^6$, $0{\cdot}44c$ and $0{\cdot}65c$ on upper and lower surfaces respectively, and at $R = 3{\cdot}4 \times 10^6$, $0{\cdot}35c$ and $0{\cdot}60c$. Curves of C_L/C_{L0} against $\log_{10} R$ for these unsymmetrical sets of values of x_T/c were found by cross-plotting Figs. 7d and 7e, which are derived by interpolation in Figs. 7a, 7b and 7c.

6. *Comparison with Royal Aeronautical Society Data Sheet.* The data sheet Wings 01.01.05 (Ref. 14), in addition to giving values of a_0 in terms of t/c and trailing-edge angle, gives curves of a_1/a_0 against $\tan \frac{1}{2}\tau$ for $R = 10^6$, 10^7 and 10^8 in the two cases of transition at the leading edge and at 50 per cent chord. These sets of curves are shown by solid lines in Figs. 9a and 9b, together with the corresponding curves from the present calculation, which are those of Figs. 4a and 4c, shown here by broken lines.

The latter lie consistently above those of the data sheet, *i.e.*, the present method predicts a smaller loss of lift. The discrepancy between the two is smaller in the leading-edge case than for $x_T/c = 0{\cdot}50$, being just inside the accuracy of $\pm$ 5 per cent assessed for the sheet in the former case and just outside for the latter.

It seems possible that the discrepancy arises from uncertainty regarding the transition point on the lower surface in the data analysed in the sheet. Examination of the sources of this data, which are listed on the sheet and include Ref. 12, shows that in many cases x_{Tl} was not known. Some values of $C_L/C_{L\,0}$ have therefore been calculated using the prescribed value for x_{Tu}, with x_{Tl} some distance further back. These are plotted as isolated points on the Figures, and indicate that a rearward movement of x_{Tl} in the calculation would bring the sets of curves into better agreement.

A further point in this connection is that the data analysed in the R.Ae.S. sheet were collected at a number of incidences. In general the transition point for a particular regime varies with incidence (as is well illustrated, for instance, in Fig. 8 of Brebner and Bagley's report), and unless the transition points are fixed independently of incidence, it is difficult to see how a single set of curves such as those of Fig. 9a can fully represent the influence of transition position.

7. *Conclusions.* It has been found possible to apply the method of Ref. 1 as a routine yielding consistent results for calculations in which a number of parameters is examined systematically. The method is straightforward in application provided the calculations are performed at an incidence small enough to render the boundary-layer calculations tractable. $\alpha = 2$ deg is found to be satisfactory for this purpose.

The method actually gives lift coefficients. Lift slopes may be deduced from these, but this involves some uncertainty regarding the movement of transition with incidence. Nevertheless, the qualitative conclusions which may be drawn from the case $\alpha = 2$ deg are likely to apply at other incidences.

REFERENCES

No.	*Author*	*Title, etc.*
1	D. A. Spence	Prediction of the characteristics of two-dimensional aerofoils. *J. Ae. Sci.* Vol. 21. No. 9. pp. 577 to 588. September, 1954.
2	J. H. Preston	The calculation of lift taking account of the boundary layer. R. & M. 2725. November, 1949.
3	H. B. Squire and A. D. Young ..	The calculation of the profile drag of aerofoils. R. & M. 1838. November, 1937.
4	W. R. Sears	Some recent developments in aerofoil theory. *J. Ae. Sci.* May, 1956.
5	R. C. Pankhurst and H. B. Squire	Calculated pressure distributions for the RAE 101–104 aerofoil sections. R.A.E. Tech. Note Aero. 2039. A.R.C. 13,254. March, 1950.
6	G. I. Taylor	Note on the connection between the lift on an aerofoil in a wind and the circulation round it. Appendix to *Phil. Trans.* A. 225. 1925. (Also printed as R. & M. 989).
7	J. H. Preston	Note on the circulation in circuits which cut the streamlines in the wake of an aerofoil at right angles. R. & M. 2957. March, 1954.
8	D. A. Spence and N. A. Routledge	Velocity calculations by conformal mapping for two-dimensional aerofoils. C.P. 241. February, 1955.
9	B. Thwaites	Approximate calculation of the laminar boundary layer. *Aero. Quart.* Vol. 1. Part III. pp. 245 to 280. November, 1949.
10	D. A. Spence	The development of turbulent boundary layers. *J. Ae. Sci.* Vol. 23. No. 1. pp. 3 to 15. January, 1956.
11	D. A. Spence	Growth of the turbulent wake close behind an aerofoil at incidence C.P. 125. May, 1952.
12	L. W. Bryant and H. C. Garner ..	Control testing in wind tunnels. R. & M. 2881. January, 1957.
13	G. G. Brebner and J. A. Bagley ..	Pressure and boundary-layer measurements on a two-dimensional wing at low speed. R. & M. 2886. February, 1952.
14	—	Royal Aeronautical Society data sheets Wings 01.01.05. January, 1956.
15	D. A. Spence	The lift coefficient of a thin, jet-flapped wing. *Proc. Roy. Soc.* A. 238. pp. 46 to 68. 1956.

APPENDIX

Circulation in the Wake

In Refs. 1 and 2 the net circulation in any segment of the wake bounded fore and aft by lines orthogonal to the streamlines, is taken to be zero. The circulation Γ_1, say, of irrotational flow past the aerofoil which, when combined with the displacement flux distribution, satisfies the condition of equal velocities at the edges of the boundary layer above and below the trailing edge, is then assumed equal to Γ_∞, and the lift is calculated at $L = \rho U_\infty \Gamma_\infty = \rho U_\infty \Gamma_1$.

In fact, however, there is in general a non-zero net circulation round an element of the wake such as that described (whose upper and lower boundaries are supposed to be streamlines outside the wake). This may be calculated by a method suggested by Preston[7], wherein it is supposed that the streamlines in such an element form concentric arcs, as in Fig. 10. If $R \mp \delta/2$ are the radii of curvature of upper and lower boundaries, on which the velocities and pressures are U_1, U_2 and p_1, p_2 respectively, and at an intermediate point the radius of curvature, velocity and pressure are respectively y, u, p, the equation for centrifugal force is

$$-\frac{dp}{dy} = \frac{\rho u^2}{y}, \tag{33}$$

where ρ is the density. Integrating across the wake

$$p_1 - p_2 = \int_{R+\delta/2}^{R-\delta/2} \frac{\rho u^2}{y}\, dy \doteq \frac{\rho}{R}\int_w u^2\, dy, \tag{34}$$

if R is large, where $\int_w$ denotes integration across the element.

Since the total head is constant outside the wake (34) may be replaced by

$$-\tfrac{1}{2}\rho(U_1^2 - U_2^2) = \frac{\rho}{R}\int_w u^2\, dy \tag{35}$$

and, since it is permissible to write approximately

$$U_1 + U_2 = 2U_\infty, \tag{36}$$

this yields

$$R(U_1 - U_2)\,U_\infty = \int u^2\, dy. \tag{37}$$

The circulation $d\Gamma_w$ (positive clockwise) round the circuit is given by

$$\begin{aligned}\frac{d\Gamma_w}{d\psi} &= U_1\left(R - \frac{\delta}{2}\right) - U_2\left(R + \frac{\delta}{2}\right)\\ &= R(U_1 - U_2) - \frac{\delta}{2}(U_1 + U_2),\end{aligned} \tag{38}$$

where ψ is the inclination of the streamlines to a fixed direction (increasing in the downstream direction).

Substituting from (37), (38) becomes

$$U_\infty \frac{d\Gamma_w}{d\psi} = \int_w u^2\, dy - \delta U_\infty^2. \tag{39}$$

If now we define displacement and momentum thicknesses for the whole wake by means of

$$U_\infty \delta_1 = \int_w (U_\infty - u)\, dy \tag{40}$$

$$U_\infty^2 \delta_2 = \int_w u(U_\infty - u)\, dy\,, \tag{41}$$

then

$$U_\infty \frac{d\Gamma_w}{d\psi} = - U_\infty^2(\delta_2 + \delta_1)\,. \tag{42}$$

Except near the trailing edge, δ_2 and δ_1 have values close to the common limit to which they tend at infinity, and we may write approximately

$$\delta_1,\ \delta_2 = \delta_{2\infty} = \tfrac{1}{2} c C_D\,, \tag{43}$$

where c is the aerofoil chord and C_D the drag coefficient. Hence

$$\frac{d\Gamma_w}{d\psi} = - c U_\infty C_D \tag{44}$$

and the total circulation is

$$\Gamma_w = - c U_\infty C_D \int_{-\alpha}^{0} d\psi = - \alpha c U_\infty C_D\,, \tag{45}$$

assuming the wake streamlines to be initially parallel to the aerofoil chord.

It might at first be thought that this circulation would simply lead to a reduction of amount $\rho U_\infty \Gamma_w$ in the total lift. But in addition to exciting this direct effect, the wake vortices induce an additional circulation, actually greater than Γ_w, round the wing itself, which results in a further loss of lift.

The effect is very similar to that of a jet-flapped wing, in which the jet operates as a vortex sheet, with strength proportional to its curvature, as in the present case, but of opposite sign, *i.e.*,

$$\frac{d\Gamma_J}{d\psi} = \tfrac{1}{2} U_\infty C_J\,, \tag{46}$$

say, where C_J is the momentum coefficient.

In that case it has been found[15] that, for small C_J, the additional lift induced by the jet sheet in the comparable case is

$$\frac{C_L(C_J)}{C_L(C_J = 0)} - 1 = \frac{\dfrac{\partial C_L}{\partial \alpha} - 2\pi}{2\pi} = 0{\cdot}151\sqrt{C_J}\,.$$

The effect of the wake is obtained by changing the sign of this term and writing $2C_D$ for C_J, *i.e.*,

$$\frac{C_L}{C_{L1}} = 1 - 0{\cdot}214\sqrt{C_D}\,,$$

where C_{L1} is the lift coefficient estimated by ignoring this effect.

It is interesting to note the balance of drag forces in this case: with the jet flap, corresponding to the vortex distribution (46) there would be a thrust C_J, so (44) gives us a drag $2C_D$. The latter, however, is partly offset by the thrust due to the displacement sources used to represent the boundary layer and wake, and the magnitude of these is precisely C_D.

TABLE 1

Variation of a_1/a_0 with Transition Position, Thickness/Chord ratio, Reynolds number and Incidence for the RAE 101 and 104 Aerofoils

RAE 101: a_1/a_0

		$\frac{X_{Tu}}{c}=0,\ \frac{X_{Tl}}{c}=0$			$\frac{X_{Tu}}{c}=0,\ \frac{X_{Tl}}{c}=0{\cdot}1$			$\frac{X_{Tu}}{c}=0,\ \frac{X_{Tl}}{c}=0{\cdot}5$		
$\frac{t}{c}$	R	10^6	10^7	10^8	10^6	10^7	10^8	10^6	10^7	10^8
0·06		0·910	0·933	0·951	0·908	0·932	0·949	0·886	0·907	0·924
0·10		0·869	0·902	0·926	0·868	0·897	0·921	0·818	0·844	0·872
0·15		0·821	0·864	0·896	0·814	0·852	0·884	0·727	0·760	0·800

		$\frac{X_{Tu}}{c}=0,\ \frac{X_{Tl}}{c}=0{\cdot}65$			$\frac{X_{Tu}}{c}=0,\ \frac{X_{Tl}}{c}=0{\cdot}80$			$\frac{X_{Tu}}{c}=0{\cdot}1,\ \frac{X_{Tl}}{c}=0{\cdot}1$		
$\frac{t}{c}$	R	10^6	10^7	10^8	10^6	10^7	10^8	10^6	10^7	10^8
0·06								0·917	0·944	0·961
0·10		0·794		0·851	0·772		0·838	0·879	0·916	0·938
0·15								0·831	0·883	0·911

		$\frac{X_{Tu}}{c}=0{\cdot}1,\ \frac{X_{Tl}}{c}=0{\cdot}5$			$\frac{X_{Tu}}{c}=0{\cdot}1,\ \frac{X_{Tl}}{c}=0{\cdot}65$			$\frac{X_{Tu}}{c}=0{\cdot}1,\ \frac{X_{Tl}}{c}=0{\cdot}80$		
$\frac{t}{c}$	R	10^6	10^7	10^8	10^6	10^7	10^8	10^6	10^7	10^8
0·06		0·894	0·918	0·933						
0·10		0·829	0·862	0·888	0·804		0·866	0·782		0·851
0·15		0·743	0·789	0·825						

		$\frac{X_{Tu}}{c}=0{\cdot}5,\ \frac{X_{Tl}}{c}=0{\cdot}5$			$\frac{X_{Tu}}{c}=0{\cdot}5,\ \frac{X_{Tl}}{c}=0{\cdot}65$			$\frac{X_{Tu}}{c}=0{\cdot}5,\ \frac{X_{Tl}}{c}=0{\cdot}80$		
$\frac{t}{c}$	R	10^6	10^7	10^8	10^6	10^7	10^8	10^6	10^7	10^8
p·06		0·947	0·970	0·978						
0·10		0·928	0·956	0·972	0·901		0·946	0·875		0·925
0·15		0·903	0·942	0·963						

		$\frac{X_{Tu}}{c} = 0{\cdot}65, \frac{X_{Tl}}{c} = 0{\cdot}65$			$\frac{X_{Tu}}{c} = 0{\cdot}65, \frac{X_{Tl}}{c} = 0{\cdot}80$			$\frac{X_{Tu}}{c} = 0{\cdot}80, \frac{X_{Tl}}{c} = 0{\cdot}80$		
$\frac{t}{c}$	R	10^6	10^7	10^8	10^6	10^7	10^8	10^6	10^7	10^8
0·06 0·10 0·15		0·938		0·978	0·911		0·952	0·945		0·986

RAE 104: a_1/a_0

		$\frac{X_{Tu}}{c} = 0{\cdot}1, \frac{X_{Tl}}{c} = 0{\cdot}1$		
$\frac{t}{c}$	R	10^6	10^7	10^8
0·06		0·906	0·934	0·951
0·10		0·862	0·901	0·925
0·15		0·804	0·857	0·894

RAE 101: a_1/a_0 $R = 10^6$, $t/c = 0{\cdot}10$

$\frac{X_{Tu}}{c}$	$\frac{X_{Tl}}{c}$	$\alpha = 2°$	$\alpha = 4°$	$\alpha = 6°$
0	0	0·869	0·869	0·868
0·50	0·50	0·928	0·925	0·920
0	0·50	0·818	0·853	0·863

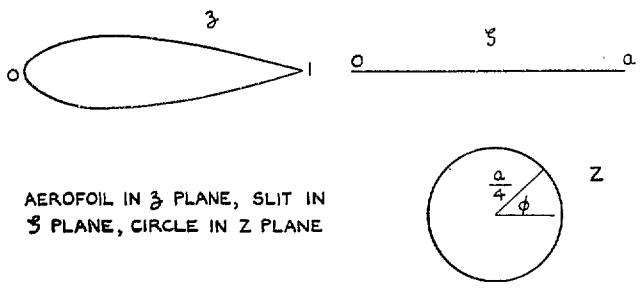

FIG. 1. Stages in transformation.

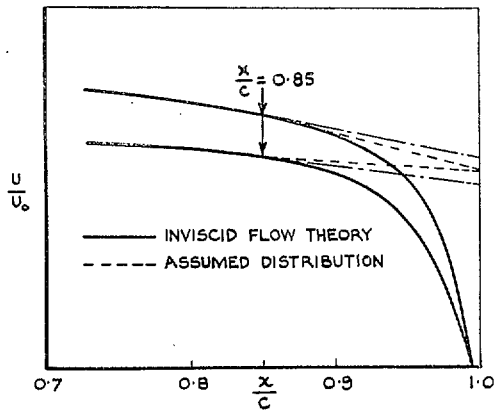

FIG. 2. Estimation of velocity distribution near the trailing edge.

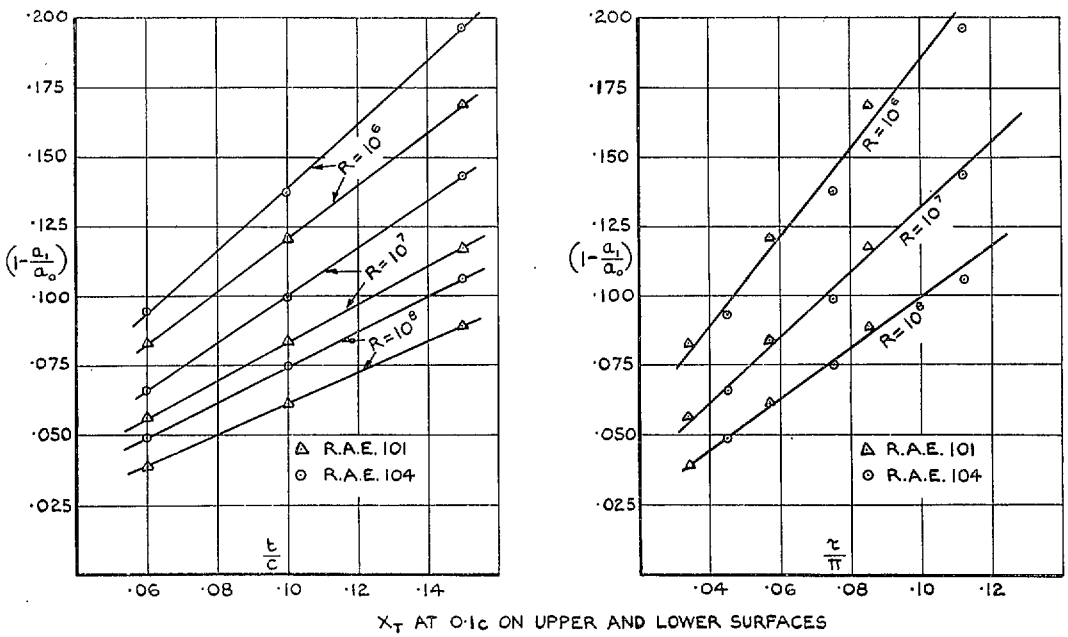

FIG. 3. Comparison of $1 - (a_1/a_0)$ for RAE 101 and 104 aerofoils.

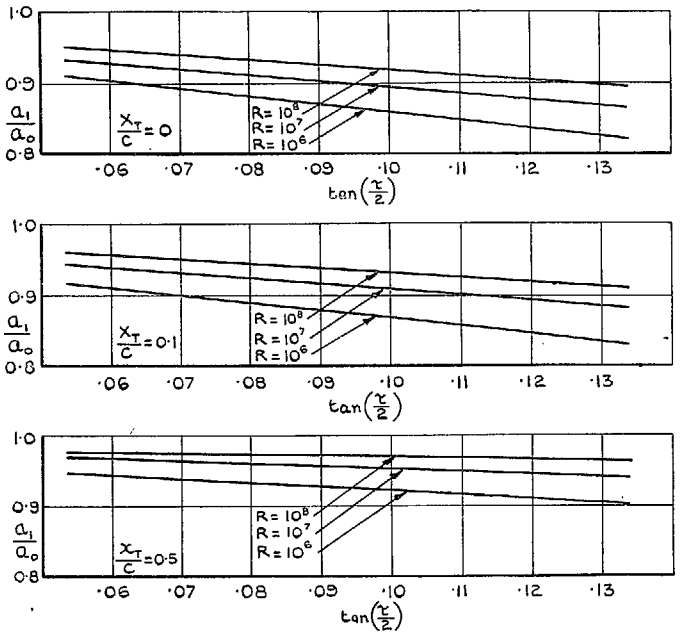

FIG. 4. RAE 101.—Variation of a_1/a_0 with trailing-edge angle (symmetrical transition).

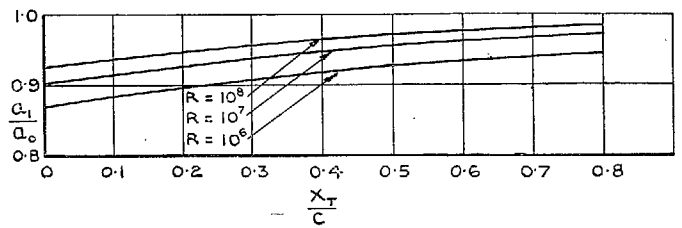

FIG. 5. RAE 101, $t/c = 0{\cdot}1$.—Variation of a_1/a_0 with (symmetrical) transition position.

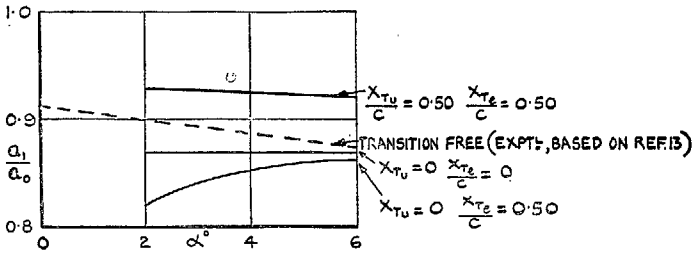

FIG. 6a. Effect of incidence upon $C_L/C_{L\,0}$.

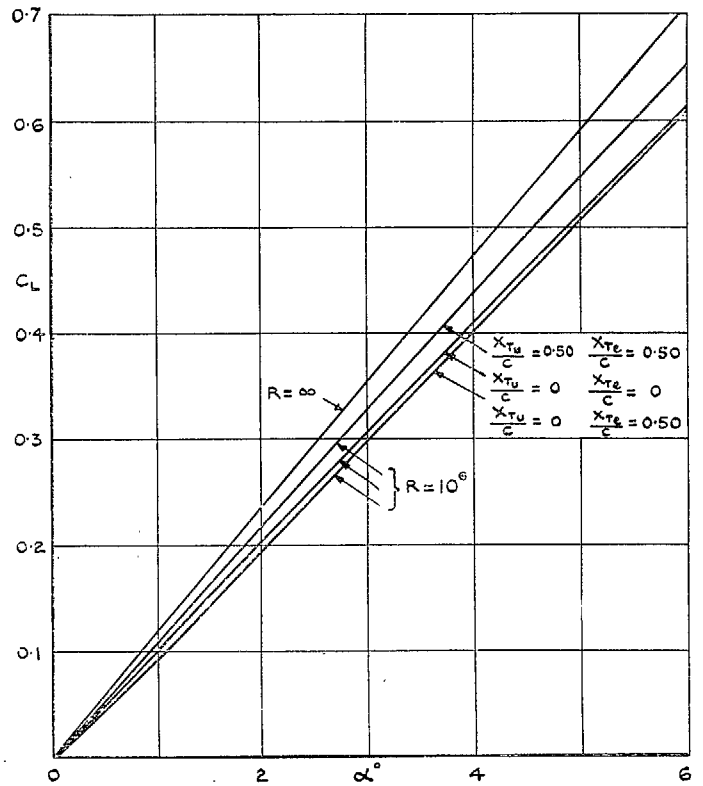

FIG. 6b. Effect of incidence upon C_L.

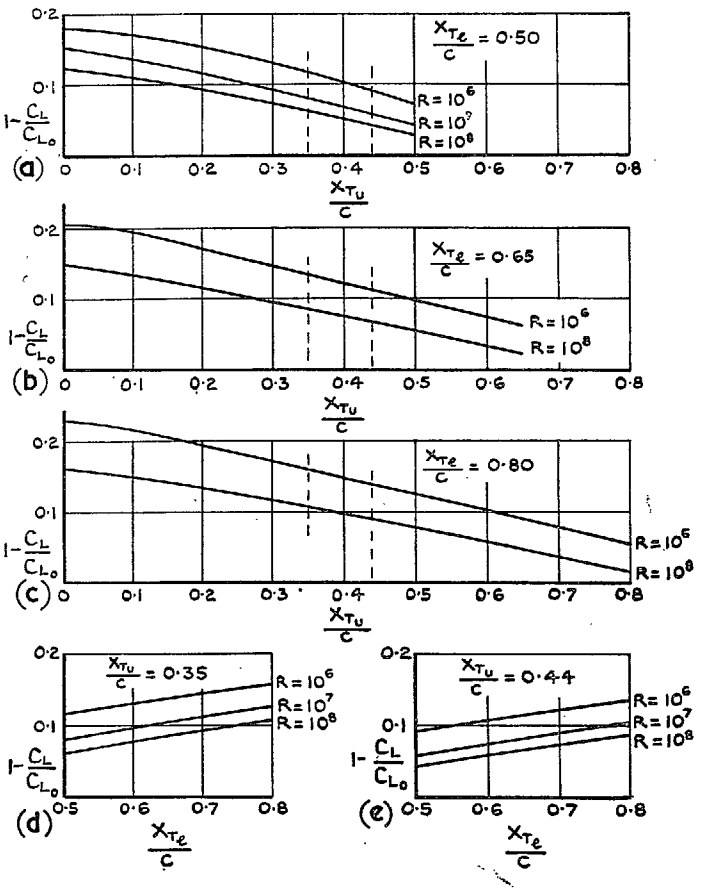

FIGS. 7a to 7e. RAE 101, $t/c = 0{\cdot}1$, $\alpha = 2$ deg.—Effect of unsymmetrical transition positions on $C_L/C_{L\,0}$.

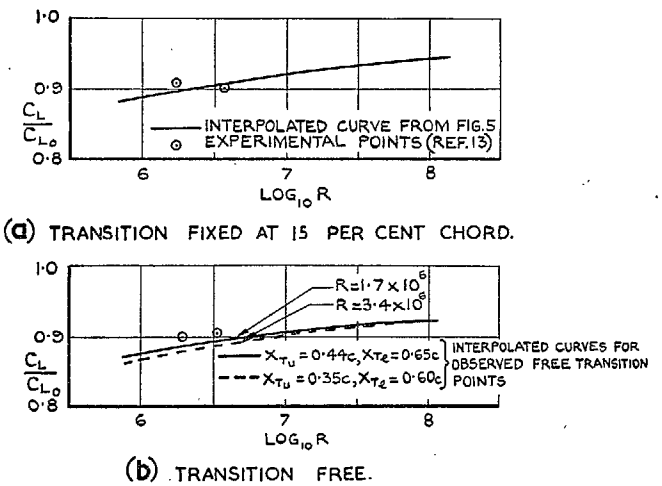

FIGS. 8a and 8b. Comparison of calculated $C_L/C_{L\,0}$ with experimental results of Ref. 13.

(78798) Wt. 54/8210 K.5 9/60 Hw.

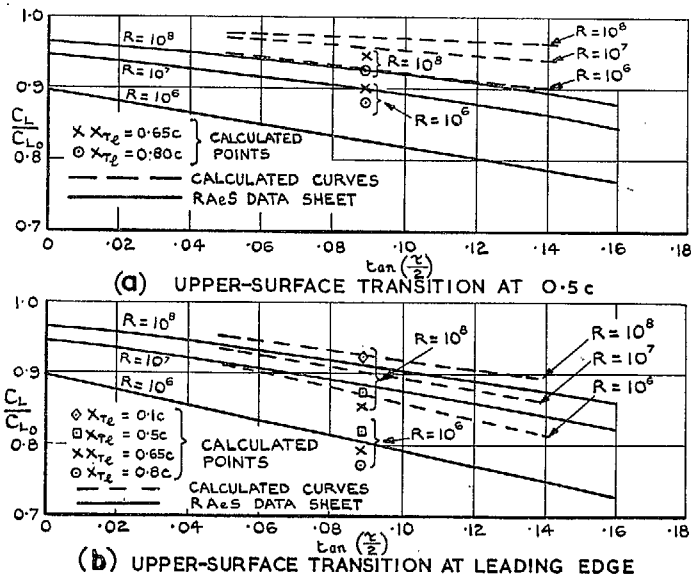

FIGS. 9a and 9b. Comparison of calculated $C_L/C_{L\,0}$ with R.Ae.S. Data sheet Wings 01.01.05.

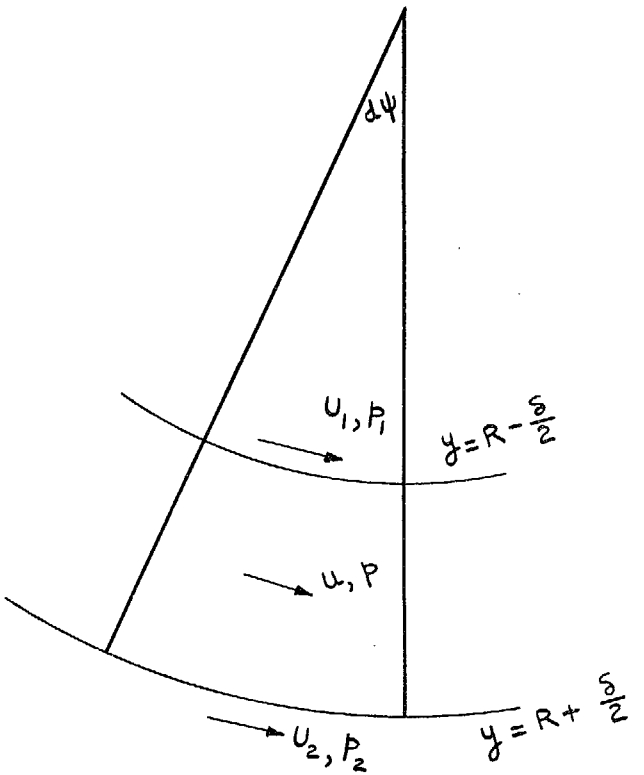

FIG. 10. Section of wake (schematic).

Publications of the Aeronautical Research Council

ANNUAL TECHNICAL REPORTS OF THE AERONAUTICAL RESEARCH COUNCIL (BOUND VOLUMES)

1941 Aero and Hydrodynamics, Aerofoils, Airscrews, Engines, Flutter, Stability and Control, Structures. 63*s.* (post 2*s.* 3*d.*)

1942 Vol. I. Aero and Hydrodynamics, Aerofoils, Airscrews, Engines. 75*s.* (post 2*s.* 3*d.*)
Vol. II. Noise, Parachutes, Stability and Control, Structures, Vibration, Wind Tunnels. 47*s.* 6*d.* (post 1*s.* 9*d.*)

1943 Vol. I. Aerodynamics, Aerofoils, Airscrews. 80*s.* (post 2*s.*)
Vol. II. Engines, Flutter, Materials, Parachutes, Performance, Stability and Control, Structures. 90*s.* (post 2*s.* 3*d.*)

1944 Vol. I. Aero and Hydrodynamics, Aerofoils, Aircraft, Airscrews, Controls. 84*s.* (post 2*s.* 6*d.*)
Vol. II. Flutter and Vibration, Materials, Miscellaneous, Navigation, Parachutes, Performance, Plates and Panels, Stability, Structures, Test Equipment, Wind Tunnels. 84*s.* (post 2*s.* 6*d.*)

1945 Vol. I. Aero and Hydrodynamics, Aerofoils. 130*s.* (post 2*s.* 9*d.*)
Vol. II. Aircraft, Airscrews, Controls. 130*s.* (post 2*s.* 9*d.*)
Vol. III. Flutter and Vibration, Instruments, Miscellaneous, Parachutes, Plates and Panels, Propulsion. 130*s.* (post 2*s.* 6*d.*)
Vol. IV. Stability, Structures, Wind Tunnels, Wind Tunnel Technique. 130*s.* (post 2*s.* 6*d.*)

Special Volumes

Vol. I. Aero and Hydrodynamics, Aerofoils, Controls, Flutter, Kites, Parachutes, Performance, Propulsion, Stability. 126*s.* (post 2*s.* 6*d.*)
Vol. II. Aero and Hydrodynamics, Aerofoils, Airscrews, Controls, Flutter, Materials, Miscellaneous, Parachutes, Propulsion, Stability, Structures. 147*s.* (post 2*s.* 6*d.*)
Vol. III. Aero and Hydrodynamics, Aerofoils, Airscrews, Controls, Flutter, Kites, Miscellaneous, Parachutes, Propulsion, Seaplanes, Stability, Structures, Test Equipment. 189*s.* (post 3*s.* 3*d.*)

Reviews of the Aeronautical Research Council

1939–48 3*s.* (post 5*d.*) 1949–54 5*s.* (post 6*d.*)

Index to all Reports and Memoranda published in the Annual Technical Reports

1909–1947 R. & M. 2600 6*s.* (post 4*d.*)

Author Index to the Reports and Memoranda and Current Papers of the Aeronautical Research Council

February, 1954–February, 1958 R. & M. No. 2570 (Revised) (Addendum) 7*s.* 6*d.* (post 4*d.*)

Indexes to the Technical Reports of the Aeronautical Research Council

July 1, 1946–December 31, 1946 R. & M. No. 2150 1*s.* 3*d.* (post 2*d.*)

Published Reports and Memoranda of the Aeronautical Research Council

Between Nos. 2251–2349	R. & M. No. 2350 1*s.* 9*d.* (post 2*d.*)
Between Nos. 2351–2449	R. & M. No. 2450 2*s.* (post 2*d.*)
Between Nos. 2451–2549	R. & M. No. 2550 2*s.* 6*d.* (post 2*d.*)
Between Nos. 2551–2649	R. & M. No. 2650 2*s.* 6*d.* (post 2*d.*)
Between Nos. 2651–2749	R. & M. No. 2750 2*s.* 6*d.* (post 2*d.*)
Between Nos. 2751–2849	R. & M. No. 2850 2*s.* 6*d.* (post 2*d.*)
Between Nos. 2851–2949	R. & M. No. 2950 3*s.* (post 2*d.*)

HER MAJESTY'S STATIONERY OFFICE

from the addresses overleaf

Printed and published by
HER MAJESTY'S STATIONERY OFFICE

To be purchased from
York House, Kingsway, London W.C.2
423 Oxford Street, London W.1
13A Castle Street, Edinburgh 2
109 St. Mary Street, Cardiff
39 King Street, Manchester 2
50 Fairfax Street, Bristol 1
2 Edmund Street, Birmingham 3
80 Chichester Street, Belfast 1
or through any bookseller

Printed in England

S.O. Code No. 23-3137